Atmos. Chem. Phys. Discuss., 13, 27201–27241, 2013
www.atmos-chem-phys-discuss.net/13/27201/2013/
doi:10.5194/acpd-13-27201-2013


Atmospheric Chemistry and Physics Discussions



# Three years of aerosol mass, black carbon and particle number concentrations at Montsec (southern Pyrenees, 1570 m a.s.l.)

**A. Ripoll**[1,2], **J. Pey**[1,*], **M. C. Minguillón**[1], **N. Pérez**[1], **M. Pandolfi**[1], **X. Querol**[1], and **A. Alastuey**[1]

[1]Institute of Environmental Assessment and Water Research (IDAEA-CSIC), Jordi Girona 18–26, 08034, Barcelona, Spain
[2]Departament d'Astronomia i Meteorologia, Universitat de Barcelona, Martí i Franquès 1, 08–28, Barcelona, Spain
[*]now at: Aix-Marseille Université, CNRS, LCE FRE 3416, Marseille, 13331, France

Received: 30 July 2013 – Accepted: 7 October 2013 – Published: 21 October 2013

Correspondence to: A. Ripoll (anna.ripoll@idaea.csic.es)

Published by Copernicus Publications on behalf of the European Geosciences Union.







## Abstract

Time variation of mass particulate matter ($PM_1$ and $PM_{1-10}$), black carbon (BC) and particle number ($N$) concentrations at the high altitude site of Montsec (MSC) in the southern Pyrenees was interpreted for the period 2010–2012.

The MSC site registered higher $PM_{10}$ ($12\,\mu g\,m^{-3}$) and $N>7$ nm ($2209\,\#\,cm^{-3}$) concentrations than those measured at other high altitude sites in central Europe ($PM_{10}$: 3–9 $\mu g\,m^{-3}$ and $N$: 634–2070 $\#\,cm^{-3}$). By contrast, BC concentrations at MSC ($0.2\,\mu g\,m^{-3}$) were equal or even lower than those measured at these European sites (0.2–0.4 $\mu g\,m^{-3}$). These differences were attributed to the lower influence of anthropogenic emissions and to the higher relevance of Saharan dust transport and new particle formation (NPF) processes at MSC.

The different time variation of PM and BC concentrations compared with that of $N$ suggests that these aerosol parameters were governed by diverse factors at MSC. Both PM and BC concentrations showed marked differences for different meteorological scenarios, with enhanced concentrations under North African outbreaks ($PM_{1-10}$: $13\,\mu g\,m^{-3}$, $PM_1$: $8\,\mu g\,m^{-3}$ and BC: $0.3\,\mu g\,m^{-3}$) and low concentrations when Atlantic advections occurred ($PM_{1-10}$: $5\,\mu g\,m^{-3}$, $PM_1$: $4\,\mu g\,m^{-3}$ and BC: $0.1\,\mu g\,m^{-3}$). Because of the contrasting origin of the air masses in the warmer seasons (spring and summer) and in the colder seasons (autumn and winter), PM and BC concentrations showed a marked increase in summer, with a secondary maximum in early spring, and were at their lowest during winter. The maximum in the warmer seasons was attributed to long-range transport processes which mask the breezes and regional transport breaking the daily cycles of these pollutants. By contrast, PM and BC concentrations showed clear diurnal cycles with maxima at midday in the colder seasons. A statistically significant weekly variation was also obtained for the BC concentrations, displaying a progressive increase from Tuesday to Saturday, followed by a significant decrease on Sunday and Monday.






ACPD
13, 27201–27241, 2013



$N$ concentrations depended more on local meteorological variables such as solar radiation than on the air mass origin. Therefore, the highest concentrations of $N$ were associated with summer regional episodes ($N > 3$ nm: 4461 # $cm^{-3}$ and $N > 7$ nm: 3021 # $cm^{-3}$) and the lowest concentrations were related to winter regional scenarios ($N > 3$ nm: 2496 # $cm^{-3}$ and $N > 7$ nm: 1073 # $cm^{-3}$). This dependence on solar radiation also accounted for the marked diurnal cycle of $N$ concentrations throughout the year with a peak at midday and for the absence of a weekly pattern.

Measurements carried out at MSC enabled us to characterize the tropospheric background aerosols in the Western Mediterranean Basin (WMB). Our results highlight the importance of the NPF processes in southern Europe, reveal much lower anthropogenic emissions than in central Europe, and underline the contribution of natural long-range transport such as Saharan dust.

## 1 Introduction

Atmospheric aerosols have been extensively investigated because of their adverse effects on health (Pope and Dockery, 2006), and because of their role in many atmospheric and climate processes, influencing the Earth's radiative balance (IPCC, 2007). Atmospheric particulate matter (PM) is associated with increasing mortality and morbidity in urban populations (Revihaap WHO, 2013). Ambient concentrations of pollutants have therefore been measured in urban areas (Eeftens et al., 2012) and have been subject to regulation (EC 2008/50/CE). Nonetheless, the effect of aerosols on climate is observed more clearly in the free troposphere (FT) than in the planetary boundary layer (PBL) because the FT is more representative of the global atmosphere (Laj et al., 2009). The reason for this is that the aerosol residence time is longer in the FT, i.e. several weeks (Kent et al., 1998). Consequently, in-situ aerosol properties are measured at high altitude mountain observatories (Asmi et al., 2013; Collaud Coen et al., 2013). Moreover, measurements at such sites enabled us to better characterize





ACPD
13, 27201–27241, 2013



background aerosols, source origins, particle formation mechanisms and long-range transport without the interference of local pollution.

Although the number of studies based on surface aerosol measurement sites worldwide is considerable, most of them have been carried out in areas within the PBL because of air quality regulations and only a few concern high elevation sites. Furthermore, the majority of these high altitude studies have been focused on greenhouse gases and aerosol radiative properties (Andrews et al., 2011; Zieger et al., 2012) whereas few studies deal with the seasonal, weekly and diurnal variation of parameters such as particle number concentration ($N$) and size distribution, black carbon (BC), and PM chemical composition, which are rising in importance (Asmi et al., 2011; Monks et al., 2009; Putaud et al., 2010).

Earlier studies at high altitude sites in Europe have been carried out in Switzerland (Jungfraujoch, 3578 m), France (Puy de Dôme, 1465 m), and Italy (Mt Cimone, 2165 m), inter alia. These studies showed a marked seasonal cycle for $PM_{10}$ (Tositti et al., 2013), BC (Marinoni et al., 2008), and $N$ (Collaud Coen et al., 2011; Venzac et al., 2009), with the lowest concentrations in winter and the highest in summer. The variation of these aerosol parameters is produced at two scales: (1) seasonal variation depending on the air mass origin and (2) daily variation controlled by PBL growth and mountain breeze transport. In contrast to central Europe, few studies on mountain aerosol have been carried out in the Western Mediterranean Basin (WMB).

The WMB is characterized by atmospheric dynamics that are atypical and complex because of its topography, the elevated emissions of anthropogenic pollutants, and the arrival of natural and anthropogenic aerosols as a result of long-range transport processes (Millan et al., 1997). All these characteristics prompted us to study the aerosol phenomenology. For this reason, a regional background aerosol monitoring station was installed at Montseny Natural Park (MSY, 720 m a.s.l.), 40 km to the N–NE of Barcelona and 25 km from the Mediterranean coast, to study the regional-scale aerosols in the WMB (Pérez et al., 2008). However, the urban and industrial contributions to the regional background aerosol concentrations in the WMB have been found to be higher





ACPD
13, 27201–27241, 2013



than those at other mountain sites in Europe (Pey et al., 2010b). Consequently, a remote aerosol measurement site was set up to gain further insight into the continental background aerosols. The site selected is in the Montsec mountain range, which is located at 1570 m a.s.l., in the southern Pyrenees, and removed from large urban and industrial areas.

In this study, the results of PM, BC and *N* measurements from a high altitude site (Montsec) are presented and they variation is interpreted. Given the location of this site between the Atlantic and the Mediterranean, greater emphasis was placed on evaluating the influence of different meteorological scenarios on these parameters. The present study seeks to: (1) evaluate the concentrations and evolution of PM, BC, and *N* at a remote site with no influence of local anthropogenic emission sources; (2) analyze the annual, seasonal, weekly, and daily variations in the concentration of continental background aerosols with respect to the MSY regional site; and (3) deduce the main factors influencing these variations.

## 2 Methodology

### 2.1 Monitoring sites

The Montsec site (MSC) is a high altitude emplacement located in the NE of the Iberian Peninsula. This station is placed at the Montsec Astronomical Observatory (Observatori Astronòmic del Montsec, OAdM) facilities, supported by the Catalan Autonomous Government and owned by the *Consorci del Montsec* (CdM). This observatory is situated at the top of the Montsec d'Ares mountain, at an altitude of 1570 m a.s.l. (42°3′ N, 0°44′ E). The Montsec mountain range has a West to East orientation and is located on the southern side of the Pyrenees, 50 km from the axial Pyrenees to the *N* (Fig. 1). This region is sparsely populated and isolated from large urban and industrial agglomerations: 140 km from Barcelona to the SE and 30 km from the largest city in the region (Balaguer, 15 769 inhabitants) to the S. Light pollution in the OAdM was found to be





ACPD
13, 27201–27241, 2013



very low (Colomé et al., 2010), which could be an indicator of the very low anthropogenic impact at this site. The station is surrounded by forest (mainly pine and oak) and Cretaceous calcareous rock formations. There is a marked prevalence, especially in the colder seasons (autumn and winter), of Atlantic advections owing its latitudinal and longitudinal position, at mid-latitude in the Ferrel cell between the sub-polar lows belt and the sub-tropical highs belt, where westerly trade winds prevail. The atmospheric dynamics is governed by the typical Mediterranean climate, with long dry periods, sporadic but intense rains, and a prevalence of local and regional atmospheric air mass circulations.

Results were compared with those simultaneously obtained at the Montseny (MSY) station, a regional background site located in the Montseny Natural Park (41°19′ N, 02°21′ E, 720 m a.s.l.), 40 km to the N–NE of the Barcelona urban area, and 25 km from the Mediterranean coast (Fig. 1). A detailed description of this site may be found in Pérez et al. (2008).

### 2.2 Sampling schedule and measurements

The MSC site consisted of a mobile laboratory equipped with aerosol monitoring instrumentation from January 2010 to August 2011. This was replaced by a permanent station in November 2011. The present paper provides results from January 2010 to December 2012. A detailed sampling schedule is shown in Fig. S1. All the meteorological data were supplied by the Catalonian Meteorological Service from the Montsec d'Ares station, which has been in operation since 2007 (Tables S1–S3, and Fig. S2) and which is also installed at the OAdM facilities. Real time PM concentrations were continuously measured by an optical counter (GRIMM 1107). PM 30 min data were daily averaged and subsequently corrected by comparison with 24 h gravimetric mass measurements of $PM_{10}$ collected every 4 days by a high volume (hi-vol) sampler. The absorption coefficient was measured continuously using a Multi Angle Absorption Photometer (MAAP, model 5012, Thermo). Equivalent BC concentrations were calculated by the MAAP instrument software by dividing the measured absorption coefficient $\sigma_{ap}$





ACPD
13, 27201–27241, 2013



($\lambda$) by 6.6 $m^2 g^{-1}$, which is the mass absorption cross section (MAC) at 637 nm (Müller et al., 2011; Petzold and Schönlinner, 2004). Absorption measurements were compared with elemental carbon (EC) determined by a SUNSET OCEC analyzer using the EUSAAR 2 protocol (Cavalli et al., 2010), in 24 h quartz filters collected with hi-vol sampler. This comparison enabled us to determine the specific MAC for this site. Nevertheless, the instrument default MAC was used to calculate BC concentrations, reported here. Measurements of particle number ($N$) concentrations were carried out using a low detection-size (3–1000 nm) condensation particle counter (TSI, CPC 3776) from January 2010 to August 2011, and an environmental (7–1000 nm) particle counter (TSI, EPC 3783) from December 2011 to December 2012 (Fig. S1).

At MSY, concentrations of PM, BC and $N$ were also measured from January 2010 to December 2012 (Fig. S1) using a GRIMM (model 180), a MAAP (model 5012) and a CPC (model 3772, 10–1000 nm), respectively. The comparison of $N$ concentrations at both sites was limited by the different size range.

### 2.3 Classification of meteorological episodes

HYSPLIT (http://www.ready.noaa.gov/HYSPLIT_traj.php), BSC/DREAM8b (http://www.bsc.es/earth-sciences/mineral-dust-forecast-system/bsc-dream8b-forecast/north-africa-europe-and-middle-ea-0), SKIRON (http://forecast.uoa.gr/dustindx.php), and NAAPS (http://www.nrlmry.navy.mil/aerosol/index_shortcuts.html) models were used to determine the transport pathways and classify the atmospheric episodes affecting the MSC. 120 h backward trajectories (for 12 a.m. modeling vertical velocity and for 3 different heights, 750, 1500 and 2500 m a.g.l) were computed on each day of measurements, and classified according to their predominant transport direction in: (1) Atlantic North (AN), (2) Atlantic North West (ANW), (3) Atlantic South West (ASW), (4) North Africa (NAF), (5) Mediterranean (MED), (6) Europe (EU), (7) Winter Regional (WREG, from November to April), and (8) Summer Regional (SREG, from May to October). The last two are characterized by regional transport from the Iberian





ACPD
13, 27201–27241, 2013



Peninsula but are divided owing to their seasonal differences. The global atmospheric circulation undergoes some seasonal oscillations, i.e. MSC is influenced by westerlies and northerlies in winter, whereas the prevailing winds come from the South in summer (Table S2 and Fig. S2). As a result, clean oceanic Atlantic advections are more frequent in winter than in summer, whereas continental NAF air masses reach this region with a higher frequency in summer than in winter (Fig. 2).

Additionally, the boundary layer height was calculated using the HYSPLIT model from the NOAA Air Resources Laboratory (http://www.ready.noaa.gov/READYamet.php), using the information for stability time series. This was calculated every three hours during the whole period (Fig. S3).

## 3 Results and discussion

### 3.1 PM, BC and *N* mean concentrations and comparison with high altitude central European sites

The mean concentrations of PM measured at MSC during the study period (2010–2012) reached 12 $\mu g\,m^{-3}$, 8 $\mu g\,m^{-3}$ and 5 $\mu g\,m^{-3}$ for $PM_{10}$, $PM_{2.5}$ and $PM_1$ respectively. These concentrations were lower than the concentrations reported at nearby regional background stations, such as Els Torms (470 m; $PM_{10}$: 14 $\mu g\,m^{-3}$, $PM_{2.5}$: 8 $\mu g\,m^{-3}$) and Cap de Creus (23 m; $PM_{10}$: 17 $\mu g\,m^{-3}$, $PM_{2.5}$: 8 $\mu g\,m^{-3}$) which are European Monitoring and Evaluation Programme (EMEP) sites, and Montseny ($PM_{10}$: 18 $\mu g\,m^{-3}$, $PM_{2.5}$: 13 $\mu g\,m^{-3}$, $PM_1$: 10 $\mu g\,m^{-3}$) (Fig. 3a). Conversely, the mean PM at MSC were higher than those obtained at other high altitude sites in central Europe, such as Jungfraujoch (Switzerland 3578 m; $PM_{10}$: 3 $\mu g\,m^{-3}$), Riji (Switzerland 1031 m; $PM_{10}$: 8 $\mu g\,m^{-3}$, $PM_{2.5}$: 7 $\mu g\,m^{-3}$, $PM_1$: 6 $\mu g\,m^{-3}$), Chaumont (Switzerland 1137 m; $PM_{10}$: 9 $\mu g\,m^{-3}$), Mt. Cimone (Italy 2165 m; $PM_{10}$: 9 $\mu g\,m^{-3}$), Vorhegg (Austria 1020 m; $PM_{10}$: 9 $\mu g\,m^{-3}$) and Schauinsland (Germany 1205 m; $PM_{10}$: 9 $\mu g\,m^{-3}$) (Fig. 3a). The difference between





ACPD
13, 27201–27241, 2013



the MSC and the nearby EMEP regional background sites could be due to the fact that the aforementioned sites are located at a lower altitude and are within the PBL. Higher concentrations at MSY were attributed to the fact that this regional site is closer to large urban agglomerations than MSC. Consequently, the anthropogenic influence is higher at MSY. The higher concentrations recorded at MSC with respect to those at other remote sites in central Europe may be due to the fact that these sites are located at higher altitudes (Jungfraujoch and Mt. Cimone) so that they are more affected by the FT conditions, or/and are much less influenced by African dust outbreaks, which is a major natural source of PM in the Mediterranean basin (Pey et al., 2013; Querol et al., 2009).

The BC three-year average concentration at MSC was 0.2 $\mu g\,m^{-3}$ (Fig. 3b), which was clearly lower than the concentrations found at MSY (0.4 $\mu g\,m^{-3}$), and equal or lower than the concentrations reported in central Europe at Schneefernerhaus (Germany 2650 m; 0.2 $\mu g\,m^{-3}$), Puy de Dôme (France 1465 m; 0.2 $\mu g\,m^{-3}$), Mt. Cimone (0.3 $\mu g\,m^{-3}$) and Schauinsland (0.4 $\mu g\,m^{-3}$). These differences could be attributed to the influence of solid fuel use for power plants and domestic heating in central Europe (Gelencsér et al., 2007), and to the fact that these central Europe stations are located downwind from important BC sources such as densely populated areas. The higher $PM_{10}$/BC ratio found at MSC (63) with respect to that at other high altitude European sites (25–49) corroborates the high influence of African dust in $PM_{10}$ concentrations at MSC.

The mean concentration of $N > 7$ nm at MSC reached 2209 $\#\,cm^{-3}$ (Fig. 3c), which was lower than the $N > 10$ nm concentrations found at MSY (3482 $\#\,cm^{-3}$), probably due to the lower anthropogenic influence at MSC. On the other hand, average $N > 7$ nm concentration at MSC was slightly higher than the average $N > 10$ nm concentrations reported at Jungfraujoch (634 $\#\,cm^{-3}$), Mt. Cimone (1847 $\#\,cm^{-3}$) and Puy de Dôme (2070 $\#\,cm^{-3}$). This difference can be partially due to the different size range of the instruments used and to the importance of NPF processes in the South of Europe. The relevant role of photochemical nucleation episodes in southern Europe as a result





ACPD
13, 27201–27241, 2013



of higher solar radiation (Cusack et al., 2013; Pey et al., 2008; Reche et al., 2011) is further confirmed by the higher $N > 3$ nm concentrations (3752 # $cm^{-3}$) with respect to the $N > 7$ nm concentrations.

Thus, at MSC, concentrations of $PM_{10}$ were higher than at high altitude sites in central Europe because of the greater influence of the Saharan dust transport affecting the Mediterranean basin (Pey et al., 2013). The effect of these episodes on $PM_{10}$ concentrations is discussed in the next section. Moreover, *N* concentrations were also higher at MSC owing to greater solar radiation favoring NPF processes. By contrast, concentrations of BC were lower because of the lower BC emissions reaching MSC.

## 3.2 Variation of PM, BC and *N* concentrations

### 3.2.1 Effects of meteorological episodes on aerosols

Backward trajectory calculations showed that the air masses that reached MSC were mainly from the Atlantic sector (Atlantic North (AN): 20 %, Atlantic North-West (ANW): 34 % and Atlantic South-West (ASW): 7 %), whereas North African (NAF) episodes occurred for 13 % of the days. Air masses from Europe (EU) reached MSC for 9 % of the time, winter regional scenarios (WREG) prevailed for 5 % of the days, and summer regional (SREG) for 7 % of the time. Mediterranean (MED) air masses were detected very infrequently (< 4 %) and therefore conclusions on their characteristics will not be drawn in the present paper.

The $PM_{1-10}$, $PM_1$, BC and *N* median concentrations were determined for the different types of episodes at MSC (Fig. 4a) and at MSY (Fig. 4b). The meteorological episodes affected all aerosol parameters similarly at both sites. The highest coarse PM mean concentration was observed at MSC under NAF influence (13 $\mu g\,m^{-3}$) which is in agreement with what was measured at MSY (Fig. 4b) (also 13 $\mu g\,m^{-3}$). This is consistent with the highest concentrations of $PM_{1-10}$ recorded during episodes of southerly winds (Fig. 5a). Furthermore, high concentrations of $PM_{1-10}$ were also measured during SREG episodes at both sites, MSC (8 $\mu g\,m^{-3}$) and MSY (9 $\mu g\,m^{-3}$).





ACPD
13, 27201–27241, 2013



The lowest concentrations of $PM_{1-10}$ were associated with the Atlantic air masses (MSC: 5 $\mu g\,m^{-3}$, MSY: 6 $\mu g\,m^{-3}$), and with the WREG scenarios (MSC: 6 $\mu g\,m^{-3}$, MSY: 5 $\mu g\,m^{-3}$) (Fig. 4). Thus, the concentrations of $PM_{1-10}$ were similar at both sites, probably as a consequence of a common origin of the coarse PM. The highest concentrations of fine PM at MSC were linked to air masses from central Europe (8 $\mu g\,m^{-3}$), North Africa (8 $\mu g\,m^{-3}$) and under SREG episodes (8 $\mu g\,m^{-3}$) (Fig. 4a), which is consistent with what was found at MSY (13 $\mu g\,m^{-3}$ for EU and NAF, and 11 $\mu g\,m^{-3}$ for SREG) (Fig. 4b). Low wind speeds were recorded at MSC during SREG episodes, Fig. 5b shows how high $PM_1$ concentrations were associated with wind velocities lower than 10 $m\,s^{-1}$. Nevertheless, whereas the lowest $PM_1$ concentrations at MSC were recorded under the Atlantic advections (4 $\mu g\,m^{-3}$) and WREG scenarios (5 $\mu g\,m^{-3}$), results at MSY did not show a specific scenario with low $PM_1$ concentrations owing to the greater influence of anthropogenic emissions affecting this site.

BC concentrations at MSC varied concurrently with those of $PM_1$, with higher concentrations observed under NAF (0.3 $\mu g\,m^{-3}$), EU (0.3 $\mu g\,m^{-3}$) and SREG (0.3 $\mu g\,m^{-3}$) episodes, and lower concentrations under Atlantic advections (0.1 $\mu g\,m^{-3}$) and WREG scenarios (0.2 $\mu g\,m^{-3}$). BC concentrations at MSY were relatively high during EU (0.5 $\mu g\,m^{-3}$) and NAF (0.5 $\mu g\,m^{-3}$) episodes. The high BC concentrations observed during NAF episodes are due to two reasons. The first reason is the possible occurrence of the simultaneous transport of African dust together with BC. The BC could be caused by wildfires in North Africa or in the Mediterranean basin (Cristofanelli et al., 2009) and/or by anthropogenic emissions from oil refineries in North Africa (Perrino et al., 2010; Rodríguez et al., 2011). A notable example of simultaneous transport of African dust and BC was recorded at MSC on 30 June 2012. Figure 6 shows how BC concentrations increased from late 29 to early 30 June at the same time as $PM_{1-10}$, and the NAAPS model reported high dust and smoke surface concentrations (Fig. 7) at MSC. The second reason concerns the interference of some mineral matter constituents in the absorption measurements, which could lead to an increase in the absorption coefficient as observed elsewhere (Vrekoussis et al., 2005). This was evident





ACPD
13, 27201–27241, 2013



at MSC during episodes where the regional pollution was much lower compared with the African dust impact (purest Saharan episodes). Figure 8 shows the absorption versus the elemental carbon (EC) concentrations determined by thermal-optical methods in 24 h filter samples as a function of the mineral matter concentration calculated by ICP-AES in the same filters. This shows that absorption and EC correlate strongly ($R^2 = 0.75$), except for the pure Saharan episodes highlighted in a yellow area and characterized by high concentrations of mineral matter, very low concentrations of EC, and abnormally high absorption. A fine example was recorded on 28–29 June 2012 (Fig. 6), when hourly concentrations of $PM_{1-10}$ increased up to 60 $\mu g\,m^{-3}$ or more, BC concentrations were about 0.4 $\mu g\,m^{-3}$, while the annual mean of BC at MSC was 0.2 $\mu g\,m^{-3}$, and the NAAPS model did not show any smoke surface concentrations affecting the Iberian Peninsula (Fig. 7). Therefore, high concentrations of mineral dust may account for high absorption values (high BC artifact), which is more evident when EC concentration is low. This could also explain why high BC concentrations were associated with southerly winds (see Fig. 5c).

*N* concentrations at MSC underwent the largest variation for these different types of episodes (wide range of concentrations) (Fig. 4a) compared with the other aerosol parameters. The higher mean *N* concentrations were reported under SREG ($N > 3$ nm: 4461 # $cm^{-3}$ and $N > 7$ nm: 3021 # $cm^{-3}$) and NAF ($N > 3$ nm: 3748 # $cm^{-3}$ and $N > 7$ nm: 2388 # $cm^{-3}$) episodes and under some Atlantic advections (ANW $N > 3$ nm: 4186 # $cm^{-3}$ and $N > 7$ nm: 2440 # $cm^{-3}$). By contrast, the lowest *N* concentrations were recorded under WREG ($N > 3$ nm: 2496 # $cm^{-3}$ and $N > 7$ nm: 1073 # $cm^{-3}$) scenarios. *N* concentrations at MSY showed a similar variation (Fig. 4b), with high concentrations associated with SREG (4382 # $cm^{-3}$), NAF (3712 # $cm^{-3}$) and Atlantic episodes (ANW: 3568 # $cm^{-3}$). However, low concentrations were not linked to a specific scenario. Thus, the highest *N* concentrations at both MSC and MSY were recorded in the warmer seasons (under SREG and NAF episodes) or when PM concentrations were low (Atlantic episodes). The high influence of enhanced photochemistry in the warmer





ACPD
13, 27201–27241, 2013



seasons and the higher frequency of NPF processes that occur during Atlantic advections could account for this inter-episode variation (Cusack et al., 2013).

Ternary plots including $PM_1$, $PM_{1-10}$, BC and $N > 3$ nm concentrations at MSC and MSY (Fig. 9a and 9b) were elaborated to better characterize the aerosol mixture during different episodes. MSC mean was characterized by lower relative BC and $PM_1$, and higher relative $PM_{1-10}$ and $N$, with respect to MSY mean. This reflected the lower anthropogenic influence and the higher relative mineral contribution at MSC. The low relative $PM_1$ and BC, and the high $N$ were more evident during Atlantic advections as a result of clean atmospheric conditions which favor NPF processes. Although $PM_1$, BC and $N$ at MSC showed a similar distribution during the remaining episodes, $PM_{1-10}$ increased from the EU episodes (with a composition similar to that of the MSY mean) to the NAF scenarios.

### 3.2.2 Seasonal variation of PM, BC and *N*

Figure 10 shows monthly averages of PM, BC and $N$ concentrations measured at MSC for the study period (2010–2012), the monthly data availability, and the annual means. A significant seasonal variation was observed in all parameters, with maximum concentrations in summer and minimum in winter, which is typical of regional background environments in the WMB (Rodríguez et al., 2003).

The summer maximum is caused by a variety of factors: (1) the summer recirculation of air masses over the western Mediterranean (Millan et al., 1997), which hinders air mass renovation and therefore favors accumulation of pollutants; (2) the higher frequency of African dust episodes (Escudero et al., 2005) (Fig. 2) over eastern Spain; (3) the lower precipitation (Table S2) that prevents atmospheric wet-scavenging processes; (4) the higher photochemistry in the atmosphere that favors the formation of secondary organic and inorganic aerosols (Querol et al., 1999); (5) the higher intensity of solar radiation that increases biogenic compound emissions (Seco et al., 2011); and (6) the increase in the PBL height (Fig. S3), which favors the mixing of atmospheric pollutants at regional scale.





ACPD
13, 27201–27241, 2013



A secondary maximum of PM and BC occurs in early spring. This secondary maximum was attributed to reasons other than those leading to the summer maximum. In spring, MSC undergoes the lowest frequency of Atlantic advections (Fig. 2), severe anthropogenic pollution episodes affecting the whole region (Pey et al., 2010a), and a seasonal peak of African dust outbreaks (Pey et al., 2013). This secondary maximum is also shown in the ternary plots as a function of monthly means (Fig. S4). A larger contribution of BC and relatively low coarse PM in February and March may be ascribed to a higher frequency of EU (Fig. 2) and regional polluting episodes. A similar behavior was observed at other mountain sites (Andrews et al., 2011).

In the colder seasons, the combination of (1) a higher frequency of occurrence and intensity of Atlantic advections (Fig. 2); (2) uncommon African dust transport (Fig. 2); and (3) a lower vertical development of the PBL, which leaves MSC in the FT on most days (Fig. S3), accounts for the markedly reduced aerosol concentrations.

$PM_{10}$ at MSC shows a more enhanced seasonal variation than $PM_1$ (Fig. 10a), with higher concentrations in the warmer seasons due to the lower precipitation in summer (Table S2) and the higher impact of African and regional resuspension of dust particles in this size fraction (Fig. 4). The seasonal behavior of BC concentrations (Fig. 10b) was very similar to that of PM, especially $PM_1$, which indicates that $PM_1$ and BC follow similar atmospheric dynamic processes at MSC. However, *N* concentrations (Fig. 10c) showed a different behavior, with a maximum in summer, probably due to the higher summer influence of regional emissions, higher photochemistry and enhanced biogenic emissions (Cusack et al., 2013). This behavior is also seen in Fig. S4.

Figure 11 shows the monthly statistics of $PM_{1-10}$, $PM_1$, BC and *N* concentrations at MSC and MSY. The monthly median of $PM_{1-10}$ and *N* concentrations are more similar between MSC and MSY than $PM_1$ and BC. Despite the differences of altitude, $PM_{1-10}$ concentrations are similar at both sites throughout the year, probably as a consequence of a common origin of the $PM_{1-10}$. Earlier studies at MSY have shown that this coarse PM is mainly of natural origin (Pey et al., 2009). $PM_1$ and BC present a different variation for each site, with lower concentrations in winter at MSC (Fig. 11a) and





ACPD
13, 27201–27241, 2013



higher amplitude of the boxes and whiskers at MSY (Fig. 11b) throughout the year. This is probably caused by the fact that MSY is considerably more influenced by winter anticyclonic pollution episodes (Pey et al., 2010a), and it is closer to the $PM_1$ and BC emission sources than MSC. Both stations have reported similar *N* concentrations despite the fact that MSC has a lower anthropogenic influence. Therefore, $PM_1$ concentrations at MSC were lower than those at MSY while *N* concentrations were similar. This confirms the major role of NPF processes, such as photochemical or/and biogenic reactions, at MSC.

### 3.2.3 Weekly patterns of PM, BC and *N*

The weekly cycle of PM and BC concentrations at MSC (Fig. 12a) showed a minimum on Sunday and Monday, whereas *N* concentrations were slightly lower during Saturday and Sunday. Fine EC, crustal elements and coarse PM concentrations showed also a minimum on Sunday and Monday at remote sites in the United States (Murphy et al., 2008). However, BC and *N* concentrations at MSY (Fig. 12b) were the lowest on Saturday and Sunday, and PM concentrations did not show a clear weekly cycle. These different weekly patterns between MSC and MSY may be ascribed to the different distances from the anthropogenic emissions. This indicates that the reduced human activity at the weekend produces a delay of one day at MSC because of the distance from large industrial and urban agglomerations, whereas the delay is only of some hours at MSY (Moreno et al., 2011). Moreover, the fact that *N* concentrations were slightly lower at the weekend but not clearly defined as a weekly cycle corroborates the view that *N* concentrations at MSC are not only associated with anthropogenic emissions but also with a local/regional non anthropogenic origin.

The data obtained from MSC for the two groups, Tuesday–Saturday and Sunday–Monday, were compared using the *Kruskal–Wallis* test (Barmet et al., 2009). A statistically significant difference (at a significance level of 5 %) between the two groups was observed only for BC ($p = 0.006$), with the lowest concentrations on Sunday–Monday compared with Tuesday–Saturday, whereas the difference was not statistically signifi-





ACPD
13, 27201–27241, 2013



cant for $PM_{1-10}$ ($p = 0.07$), $PM_1$ ($p = 0.16$) and $N$ ($p = 0.5$). Comparison of Monday–Friday and Saturday–Sunday $N$ concentrations at MSC showed no statistically significant differences ($p = 0.17$) either.

### 3.2.4 Daily patterns of PM, BC and *N*

The diurnal cycle of PM (Fig. 13a) and BC (Fig. 13b) concentrations was less pronounced than that of $N$ (Fig. 13c) concentrations at MSC, which demonstrates that the variation of these aerosol parameters depends on a variety of factors. The hourly variation of $PM_{1-10}$ and $PM_1$ as well as that of BC was driven by mountain breezes and synoptic circulations, whereas that of $N$ depended on the solar radiation cycle rather than on air mass origin.

In the warmer seasons $PM_1$, $PM_{1-10}$ and BC (Fig. 13a, b) concentrations showed no clear diurnal patterns, which is consistent with the findings obtained for the aerosol particle composition at the Puy-de-Dôme station (Freney et al., 2011). Conversely, at MSY concentrations of PM, BC and $N$ showed clear daily patterns throughout the year (Cusack et al., 2013; Pérez et al., 2008) (Fig. S5). The lack of a defined daily pattern in the warmer seasons at MSC could be due to the combination of different phenomena, i.e. (1) the highest frequency of Saharan dust intrusions from North Africa (Fig. 2) associated with high concentrations of $PM_{1-10}$ and BC during the day and at night; (2) the widespread occurrence of wildfires around the WMB; (3) the relatively high frequency of European polluted episodes in spring (Fig. 2), both scenarios being linked to high concentrations of $PM_1$ and BC during the day and at night; and (4) the summer recirculation over the WMB, which creates a continuous increase in the background concentrations of PM and BC. Such recirculation induced by an abrupt orography causes the formation of reserve strata at a relatively high altitude (Millan et al., 1997), which could be persistent at night, increasing nocturnal concentrations of PM and avoiding the definition of clear daily cycles. The occurrence of African dust outbreaks, which are more intense at higher altitude sites during specific episodes, could also interfere with the daily pattern of PM since PM concentrations could increase during these episodes





ACPD
13, 27201–27241, 2013



regardless of the time of the day (see Fig. 6). Hence, the diurnal variation of PM and BC at MSC in the warmer seasons is dominated by the synoptic circulation, which masks the mountain breezes and the regional transport.

By contrast, in the colder seasons PM and BC concentrations showed strongest diurnal variation, with a minimum at night and a maximum around 14:00–16:00 UTC. This behavior is probably because MSC is located most of the day within the FT in the colder seasons, whereas PBL air mass is usually only advected to the site during the central hours of the day (Fig. S3). Moreover, thermal inversions are very frequent from 20:00 to 07:00 UTC. These situations prevent the transport of pollutants from the most populated areas towards high altitudes, especially at night. In the morning, mountain breezes develop, with an intensity sufficient to transport the pollutants from the adjacent valleys and plains to the top of the mountain arriving later in the afternoon. Similar phenomena have been observed at Jungfraujoch (Baltensperger et al., 1997), Mt. Cimone (Marinoni et al., 2008), Himalayas (Marinoni et al., 2010), and Puy-de-Dôme (Freney et al., 2011). Mountain breezes therefore play an important role in determining the diurnal variation of PM and BC in the colder seasons at MSC. However, the long-range transport of atmospheric pollutants also accounts for the PM and BC in these seasons. The main difference is that the synoptic circulation in the colder seasons causes the transport of clean air masses from the Atlantic for about 70 % of the days, (whereas this proportion reaches only 55 % in the warmer seasons). These air masses are associated with increased precipitation and intense winds (Table S2 and Fig. S2), leading to low concentrations of PM pollutants (Fig. 4).

*N* concentrations had a markedly daily pattern throughout the year (Fig. 13c), with the highest concentrations between 12:00 and 16:00 UTC and the lowest at night and in the early morning. This behavior is similar to that obtained at other mountain sites such as Puy de Dôme (Venzac et al., 2009). In this study, the marked daily pattern was attributed to the height development of the PBL and to the higher frequency of new particle events. At MSC, the increase in *N* concentrations during the day throughout the year suggests local/regional processes governing *N* variation since the daily





ACPD
13, 27201–27241, 2013



pattern was independent of the synoptic conditions. Moreover, the diurnal cycle of $N$ concentrations (Fig. 13c) is clearly related to that of solar radiation intensity since both parameters peak almost at the same time. $N$ peak concentrations are also associated with moderate southwesterlies (usually lower than $5\,m\,s^{-1}$) (Fig. 5d, e), which prevail from midday to early afternoon (16:00 UTC) during which time maximum solar radiation intensity is recorded. This pattern indicates a strong dependence of $N$ on solar radiation, which could be linked to a photochemical nucleation process. Despite the marked diurnal cycle throughout the year, the daily amplitude of $N$ concentrations was lower in the colder seasons than in the warmer seasons. This difference is more evident for $N > 3$ nm than for $N > 7$ nm concentrations. At night (20:00–07:00 UTC), $N > 3$ nm concentrations were more than $2100\,\#\,cm^{-3}$ in the warmer seasons, whereas they were about $1300\,\#\,cm^{-3}$ in the colder seasons. Moreover, during the day (08:00–19:00 UTC) the $N > 3$ nm concentrations rose to $7000\,\#\,cm^{-3}$ in the warmer seasons, whereas they reached $2300\,\#\,cm^{-3}$ in the colder seasons. The daily ratios between day and night mean concentrations ranged from 2.4–2 in the colder seasons to 2.9–2.8 in the warmer seasons. This seasonal variation could be associated with the fact that MSC is frequently in the FT in the colder seasons and the biogenic emissions and the photochemistry are enhanced by high solar radiation intensity in the warmer seasons, which favors NPF processes (Cusack et al., 2013). The higher $N > 3$ nm concentrations at midday with respect to the $N > 7$ nm concentrations further confirmed the relevant role of nucleation episodes at MSC. The high background $N$ concentrations in the warmer seasons could be ascribed to the recirculation transport that accumulates regional pollutants nearby, before transport by mountain breezes.

## 4 Conclusions

Aerosol parameters (PM, BC and $N$) and their variations were studied during 2010–2012 at a high altitude site (Montsec) in the southern Pyrenees. Comparison of our data with those from other high altitude sites in central Europe shows that Saharan





ACPD
13, 27201–27241, 2013



dust transport is much more important at MSC. This is corroborated by the more elevated $PM_{10}$ concentrations. The higher $N$ concentrations at MSC are due to a greater solar radiation that favors NPF processes. Conversely, BC concentrations are lower at MSC than at other sites in Europe probably because of the lower BC emissions surrounding the site. The variations of PM and BC concentrations with respect to those of $N$ demonstrated that these aerosol parameters are governed by various factors.

PM and BC show marked differences in mean concentrations for different meteorological episodes, the most polluted being the NAF air masses and the least polluted being the Atlantic advections. NAF air masses transport essentially Saharan dust, which increases PM, in addition to smoke particles from wildfires and/or anthropogenic emissions that enhance BC concentrations. In some cases, it has been shown that mineral dust components interfere with absorption measurements, leading to increased BC concentrations. SREG and EU air masses were also identified as "polluted scenarios". Atlantic advections and WREG episodes lead to the lowest concentrations of PM and BC because of the cleansing effect of the Atlantic air masses and because of the longer time spent by MSC in the FT during WREG episodes.

Seasonal variation of PM and BC concentrations was also observed, with maximum concentrations in summer and minimum concentrations in winter. This was attributed to changes in the air mass origin from summer to winter, and to the different PBL height between seasons. However, $PM_{10}$ concentrations showed more enhanced seasonal variation than $PM_1$ and BC because coarse PM is more affected by NAF episodes and to a lesser degree by regional resuspension of dust. $PM_1$ and BC concentrations were more associated with an anthropogenic origin which had a seasonal variation that was less marked, albeit a greater weekly influence. The reduced human activity at the weekend is reflected in the concentrations of $PM_1$ and BC with a delay of one day (minimum on Sunday and Monday), which confirms that MSC is located at a sufficient distance from anthropogenic emissions. Nevertheless, only BC concentrations showed a statistically significant weekly variation. Daily patterns of these parameters were also studied for each month. The hourly variations of PM and BC concentrations





ACPD
13, 27201–27241, 2013



were driven by mountain breezes and synoptic circulations. However, the long-range transport masks the breezes and regional transport breaking the daily cycles in the warmer seasons, whereas the mountain breezes had a greater impact than the synoptic circulation in the colder seasons, which is reflected in clearer diurnal patterns.

*N* concentrations were less affected by the air mass pathway and depended more on meteorological variables such as solar radiation. Even so, under NAF and SREG episodes, *N* concentrations were also relatively high, because NAF episodes were more frequent in the warmer (18 %) than in the colder (7 %) seasons, and in these warm seasons NPF processes could be enhanced because of the higher photochemistry and biogenic emissions. Furthermore, under the influence of the Atlantic advections, MSC yielded high concentrations of *N* because of the clean atmospheric conditions, which favor NPF processes as well. Seasonal variation of *N* concentrations showed a minimum in winter and a maximum in summer, which was attributed to the seasonal variation of the meteorological conditions and to the different PBL height between seasons. The undefined weekly pattern of *N* concentrations lent further support to the view that *N* concentrations are more associated with a local/regional non anthropogenic origin than with an anthropogenic origin. In addition, the *N* diurnal pattern proved to be independent of the air mass origin and followed the solar radiation cycle. Despite the daily cycle throughout the year, the daily amplitude and the background *N* concentrations were higher in the warmer than in the colder seasons. This seasonal variation was related to the higher NPF episodes and to the increased emission intensity within the PBL in the warmer seasons.

The results obtained at MSC allowed us to characterize the tropospheric background aerosols in the WMB. They are representative of a wide area and could be of interest in the investigation of the radiative balance of aerosols in SW Europe. These results: (1) confirm a lower regional anthropogenic influence at MSC than at MSY; (2) highlight the importance of the NPF processes in SW Europe because of higher solar radiation which increases photochemistry and biogenic emissions; (3) reveal much lower anthropogenic emissions than in central Europe; and (4) underline the contribution of





ACPD
13, 27201–27241, 2013



long-range transport, especially Saharan dust. All these processes could alter optical properties of aerosols and could therefore exert a significant influence on the radiative forcing. For this reason, aerosol chemical composition and scattering properties were also measured at this site. The results obtained will be discussed in forthcoming publications.

**Supplementary material related to this article is available online at http://www.atmos-chem-phys-discuss.net/13/27201/2013/acpd-13-27201-2013-supplement.pdf.**

*Acknowledgements.* This study was supported by the Ministry of Economy and Competitiveness and FEDER funds under the PRISMA (CGL2012-39623-C02-0), VAMOS (CGL2010 19464/CLI), CARIATI (CGL2008-06294/CLI), and GRACCIE (CSD 2007-00067) projects. This work was partially funded by Generalitat de Catalunya 2009 SGR8. The research received funding from the European Union Seventh Framework Programme (FP7/2007-2013) ACTRIS under grant agreement no. 262254. The authors would like to extend their gratitude to the personnel form the OAdM. We would also like to express our gratitude to METEOCAT for the meteorological data, to ACTRIS Data Center for the data from the high altitude central European sites, to the Laboratory of Atmospheric Chemistry at Paul Scherrer Institute for providing the Jungfraujoch BC and *N* data, the International Foundation High Altitude Research Stations Jungfraujoch and Gornergrat (HFSJG), and the support by MeteoSwiss within the Swiss program of the WMO Global Atmosphere Watch (GAW), to the NABEL (FOEN/Empa) for providing the PM data from the Swiss sites, to the background monitoring network of Umweltbundesamt, Vienna, for providing the Vorhegg $PM_{10}$ data, to the OPGC (Observatoire de Physique du Globe de Clermont-Ferrand) for providing the Puy de Dôme BC and *N* data, and to the NOAA Air Resources Laboratory (ARL) for the provision of the HYSPLIT transport and dispersion model, and boundary layer height calculation, used in this publication. M.C. Minguillón was funded by JAE-Doc CSIC program, co-funded by the European Social Fund (ESF).





ACPD
13, 27201–27241, 2013



## References


Andrews, E., Ogren, J. A., Bonasoni, P., Marinoni, A., Cuevas, E., Rodríguez, S., Sun, J. Y., Jaffe, D. A., Fischer, E. V., Baltensperger, U., Weingartner, E., Collaud Coen, M., Sharma, S., Macdonald, A. M., Leaitch, W. R., Lin, N.-H., Laj, P., Arsov, T., Kalapov, I., Jefferson, A., and Sheridan, P.: Climatology of aerosol radiative properties in the free troposphere, Atmos. Res., 102, 365–393, doi:10.1016/j.atmosres.2011.08.017, 2011.

Asmi, A., Wiedensohler, A., Laj, P., Fjaeraa, A.-M., Sellegri, K., Birmili, W., Weingartner, E., Baltensperger, U., Zdimal, V., Zikova, N., Putaud, J.-P., Marinoni, A., Tunved, P., Hansson, H.-C., Fiebig, M., Kivekäs, N., Lihavainen, H., Asmi, E., Ulevicius, V., Aalto, P. P., Swietlicki, E., Kristensson, A., Mihalopoulos, N., Kalivitis, N., Kalapov, I., Kiss, G., de Leeuw, G., Henzing, B., Harrison, R. M., Beddows, D., O'Dowd, C., Jennings, S. G., Flentje, H., Weinhold, K., Meinhardt, F., Ries, L., and Kulmala, M.: Number size distributions and seasonality of submicron particles in Europe 2008–2009, Atmos. Chem. Phys., 11, 5505–5538, doi:10.5194/acp-11-5505-2011, 2011.

Asmi, A., Collaud Coen, M., Ogren, J. A., Andrews, E., Sheridan, P., Jefferson, A., Weingartner, E., Baltensperger, U., Bukowiecki, N., Lihavainen, H., Kivekäs, N., Asmi, E., Aalto, P. P., Kulmala, M., Wiedensohler, A., Birmili, W., Hamed, A., O'Dowd, C., G Jennings, S., Weller, R., Flentje, H., Fjaeraa, A. M., Fiebig, M., Myhre, C. L., Hallar, A. G., Swietlicki, E., Kristensson, A., and Laj, P.: Aerosol decadal trends – Part 2: In-situ aerosol particle number concentrations at GAW and ACTRIS stations, Atmos. Chem. Phys., 13, 895–916, doi:10.5194/acp-13-895-2013, 2013.

Baltensperger, U., Gfiggeler, H. W., Jost, D. T., Lugauer, M., Schwikowski, M., and Weingartner, E.: Aerosol climatology at the high-alpine site Jungfraujoch, Switzerland, J. Geophys. Res., 102, 19707–19715, doi:10.1029/97JD00928, 1997.

Barmet, P., Kuster, T., Muhlbauer, A., and Lohmann, U.: Weekly cycle in particulate matter versus weekly cycle in precipitation over Switzerland, J. Geophys. Res., 114, D05206, doi:10.1029/2008JD011192, 2009.

Cavalli, F., Viana, M., Yttri, K. E., Genberg, J., and Putaud, J.-P.: Toward a standardised thermal-optical protocol for measuring atmospheric organic and elemental carbon: the EUSAAR protocol, Atmos. Meas. Tech., 3, 79–89, doi:10.5194/amt-3-79-2010, 2010.

Collaud Coen, M., Weingartner, E., Furger, M., Nyeki, S., Prévôt, A. S. H., Steinbacher, M., and Baltensperger, U.: Aerosol climatology and planetary boundary influence at the Jungfraujoch






ACPD
13, 27201–27241, 2013



analyzed by synoptic weather types, Atmos. Chem. Phys., 11, 5931–5944, doi:10.5194/acp-11-5931-2011, 2011.

Collaud Coen, M., Andrews, E., Asmi, A., Baltensperger, U., Bukowiecki, N., Day, D., Fiebig, M., Fjaeraa, A. M., Flentje, H., Hyvärinen, A., Jefferson, A., Jennings, S. G., Kouvarakis, G., Lihavainen, H., Lund Myhre, C., Malm, W. C., Mihapopoulos, N., Molenar, J. V., O'Dowd, C., Ogren, J. A., Schichtel, B. A., Sheridan, P., Virkkula, A., Weingartner, E., Weller, R., and Laj, P.: Aerosol decadal trends – Part 1: In-situ optical measurements at GAW and IMPROVE stations, Atmos. Chem. Phys., 13, 869–894, doi:10.5194/acp-13-869-2013, 2013.

Colomé, J., Ribas, I., Francisco, X., Casteels, K., Fernández, D., Isern, J., Palau, X., and Torra, J.: The OAdM Robotic Observatory, Adv. Astronom., 2010, 1–8, doi:10.1155/2010/183016, 2010.

Cristofanelli, P., Marinoni, A., Arduini, J., Bonafè, U., Calzolari, F., Colombo, T., Decesari, S., Duchi, R., Facchini, M. C., Fierli, F., Finessi, E., Maione, M., Chiari, M., Calzolai, G., Messina, P., Orlandi, E., Roccato, F., and Bonasoni, P.: Significant variations of trace gas composition and aerosol properties at Mt. Cimone during air mass transport from North Africa – contributions from wildfire emissions and mineral dust, Atmos. Chem. Phys., 9, 4603–4619, doi:10.5194/acp-9-4603-2009, 2009.

Cusack, M., Pérez, N., Pey, J., Wiedensohler, A., Alastuey, A., and Querol, X.: Variability of sub-micrometer particle number size distributions and concentrations in the Western Mediterranean regional background, Tellus B, 65, 1–19, 2013.

EC: Directive 2008/50/EC of the European Parliament and of the Council of 21 May 2008 on ambient air quality and cleaner air for Europe (OJ L 152, 11.6.2008), 1–44, available at: http://eur-lex.europa.eu/LexUriServ/LexUriServ.do?uri=OJ:L:2008:152:0001:0044:EN:PDF (last access: 17 October 2013), 2008.

Eeftens, M., Tsai, M.-Y., Ampe, C., Anwander, B., Beelen, R., Bellander, T., Cesaroni, G., Cirach, M., Cyrys, J., De Hoogh, K., De Nazelle, A., De Vocht, F., Declercq, C., Dėdelė, A., Eriksen, K., Galassi, C., Gražulevièienė, R., Grivas, G., Heinrich, J., Hoffmann, B., Iakovides, M., Ineichen, A., Katsouyanni, K., Korek, M., Krämer, U., Kuhlbusch, T., Lanki, T., Madsen, C., Meliefste, K., Mölter, A., Mosler, G., Nieuwenhuijsen, M., Oldenwening, M., Pennanen, A., Probst-Hensch, N., Quass, U., Raaschou-Nielsen, O., Ranzi, A., Stephanou, E., Sugiri, D., Udvardy, O., Vaskövi, É., Weinmayr, G., Brunekreef, B., and Hoek, G.: Spatial variation of $PM_{2.5}$, $PM_{10}$, $PM_{2.5}$ absorbance and PMcoarse concentrations between and within





ACPD
13, 27201–27241, 2013



20 European study areas and the relationship with $NO_2$ – results of the ESCAPE project, Atmos. Environ., 62, 303–317, doi:10.1016/j.atmosenv.2012.08.038, 2012.
Escudero, M., Castillo, S., Querol, X., Avila, A., Alarco, M., Alastuey, A., Cuevas, E., and Rodríguez, S.: Wet and dry African dust episodes over eastern Spain, J. Geophys. Res., 110, D18S08, doi:10.1029/2004JD004731, 2005.
Freney, E. J., Sellegri, K., Canonaco, F., Boulon, J., Hervo, M., Weigel, R., Pichon, J. M., Colomb, A., Prévôt, A. S. H., and Laj, P.: Seasonal variations in aerosol particle composition at the puy-de-Dôme research station in France, Atmos. Chem. Phys., 11, 13047–13059, doi:10.5194/acp-11-13047-2011, 2011.
Gelencsér, A., May, B., Simpson, D., Sánchez-Ochoa, A., Kasper-Giebl, A., Puxbaum, H., Caseiro, A., Pio, C., and Legrand, M.: Source apportionment of $PM_{2.5}$ organic aerosol over Europe: Primary/secondary, natural/anthropogenic, and fossil/biogenic origin, J. Geophys. Res., 112, D23S04, doi:10.1029/2006JD008094, 2007.
IPCC: Climate Change 2007: Synthesis Report, Contribution of Working Groups I, II and III to the Fourth Assessment Report of the Intergovernmental Panel on Climate Change [Core Writing Team, edietd by: Pachauri, R. K. and Reisinger, A., IPCC, Geneva, Switzerland, 104 pp., 2007.
Kent, G. S., Trepte, C. R., and Lucker, P. L.: Long-term stratospheric aerosol and gas experiment I and II measurements of upper tropospheric aerosol extinction, J. Geophys. Res., 103, 28863, doi:10.1029/98JD02583, 1998.
Laj, P., Klausen, J., Bilde, M., Plaß-Duelmer, C., Pappalardo, G., Clerbaux, C., Baltensperger, U., Hjorth, J., Simpson, D., Reimann, S., Coheur, P.-F., Richter, A., De Mazière, M., Rudich, Y., McFiggans, G., Torseth, K., Wiedensohler, A., Morin, S., Schulz, M., Allan, J. D., Attié, J.-L., Barnes, I., Birmili, W., Cammas, J. P., Dommen, J., Dorn, H.-P., Fowler, D., Fuzzi, S., Glasius, M., Granier, C., Hermann, M., Isaksen, I. S. A., Kinne, S., Koren, I., Madonna, F., Maione, M., Massling, A., Moehler, O., Mona, L., Monks, P. S., Müller, D., Müller, T., Orphal, J., Peuch, V.-H., Stratmann, F., Tanré, D., Tyndall, G., Abo Riziq, A., Van Roozendael, M., Villani, P., Wehner, B., Wex, H., and Zardini, A. A.: Measuring atmospheric composition change, Atmos. Environ., 43, 5351–5414, doi:10.1016/j.atmosenv.2009.08.020, 2009.
Marinoni, A., Cristofanelli, P., Calzolari, F., Roccato, F., Bonafè, U., and Bonasoni, P.: Continuous measurements of aerosol physical parameters at the Mt. Cimone GAW Station





ACPD
13, 27201–27241, 2013



(2165 m a.s.l., Italy), Sci. Total. Environ., 391, 241–51, doi:10.1016/j.scitotenv.2007.10.004, 2008.
Marinoni, A., Cristofanelli, P., Laj, P., Duchi, R., Calzolari, F., Decesari, S., Sellegri, K., Vuillermoz, E., Verza, G. P., Villani, P., and Bonasoni, P.: Aerosol mass and black carbon concentrations, a two year record at NCO-P (5079 m, Southern Himalayas), Atmos. Chem. Phys., 10, 8551–8562, doi:10.5194/acp-10-8551-2010, 2010.
Millan, M. M., Salvador, R., Mantilla, E., and Kallos, G.: Photooxidant dynamics in the Mediterranean basin in summer: results from European research projects, J. Geophys. Res., 102, 8811–8823, 1997.
Monks, P. S., Granier, C., Fuzzi, S., Stohl, A., Williams, M. L., Akimoto, H., Amann, M., Baklanov, A., Baltensperger, U., Bey, I., Blake, N., Blake, R. S., Carslaw, K., Cooper, O. R., Dentener, F., Fowler, D., Fragkou, E., Frost, G. J., Generoso, S., Ginoux, P., Grewe, V., Guenther, A., Hansson, H. C., Henne, S., Hjorth, J., Hofzumahaus, A., Huntrieser, H., Isaksen, I. S. A., Jenkin, M. E., Kaiser, J., Kanakidou, M., Klimont, Z., Kulmala, M., Laj, P., Lawrence, M. G., Lee, J. D., Liousse, C., Maione, M., McFiggans, G., Metzger, A., Mieville, A., Moussiopoulos, N., Orlando, J. J., O'Dowd, C. D., Palmer, P. I., Parrish, D. D., Petzold, A., Platt, U., Pöschl, U., Prévôt, A. S. H., Reeves, C. E., Reimann, S., Rudich, Y., Sellegri, K., Steinbrecher, R., Simpson, D., Ten Brink, H., Theloke, J., Van der Werf, G. R., Vautard, R., Vestreng, V., Vlachokostas, C., and Von Glasow, R.: Atmospheric composition change – global and regional air quality, Atmos. Environ., 43, 5268–5350, doi:10.1016/j.atmosenv.2009.08.021, 2009.
Moreno, T., Querol, X., Alastuey, A., Reche, C., Cusack, M., Amato, F., Pandolfi, M., Pey, J., Richard, A., Prévôt, A. S. H., Furger, M., and Gibbons, W.: Variations in time and space of trace metal aerosol concentrations in urban areas and their surroundings, Atmos. Chem. Phys., 11, 9415–9430, doi:10.5194/acp-11-9415-2011, 2011.
Müller, T., Henzing, J. S., de Leeuw, G., Wiedensohler, A., Alastuey, A., Angelov, H., Bizjak, M., Collaud Coen, M., Engström, J. E., Gruening, C., Hillamo, R., Hoffer, A., Imre, K., Ivanow, P., Jennings, G., Sun, J. Y., Kalivitis, N., Karlsson, H., Komppula, M., Laj, P., Li, S.-M., Lunder, C., Marinoni, A., Martins dos Santos, S., Moerman, M., Nowak, A., Ogren, J. A., Petzold, A., Pichon, J. M., Rodriquez, S., Sharma, S., Sheridan, P. J., Teinilä, K., Tuch, T., Viana, M., Virkkula, A., Weingartner, E., Wilhelm, R., and Wang, Y. Q.: Characterization and intercomparison of aerosol absorption photometers: result of two intercomparison workshops, Atmos. Meas. Tech., 4, 245–268, doi:10.5194/amt-4-245-2011, 2011.





ACPD
13, 27201–27241, 2013



Murphy, D. M., Capps, S. L., Daniel, J. S., Frost, G. J., and White, W. H.: Weekly patterns of aerosol in the United States, Atmos. Chem. Phys., 8, 2729–2739, doi:10.5194/acp-8-2729-2008, 2008.

Pérez, N., Pey, J., Castillo, S., Viana, M., Alastuey, A and Querol, X.: Interpretation of the variability of levels of regional background aerosols in the Western Mediterranean., Sci. Total Environ., 407, 527–40, doi:10.1016/j.scitotenv.2008.09.006, 2008.

Perrino, C., Canepari, S., Pappalardo, S., and Marconi, E.: Time-resolved measurements of water-soluble ions and elements in atmospheric particulate matter for the characterization of local and long-range transport events, Chemosphere, 80, 1291–300, doi:10.1016/j.chemosphere.2010.06.050, 2010.

Petzold, A. and Schönlinner, M.: Multi-angle absorption photometry – a new method for the measurement of aerosol light absorption and atmospheric black carbon, J. Aerosol Sci., 35, 421–441, doi:10.1016/j.jaerosci.2003.09.005, 2004.

Pey, J., Rodríguez, S., Querol, X., Alastuey, A., Moreno, T., Putaud, J. P., and Van Dingenen, R.: Variations of urban aerosols in the western Mediterranean, Atmos. Environ., 42, 9052–9062, doi:10.1016/j.atmosenv.2008.09.049, 2008.

Pey, J., Pérez, N., Castillo, S., Viana, M., Moreno, T., Pandolfi, M., López-Sebastián, J. M., Alastuey, A., and Querol, X.: Geochemistry of regional background aerosols in the Western Mediterranean, Atmos. Res., 94, 422–435, doi:10.1016/j.atmosres.2009.07.001, 2009.

Pey, J., Pérez, N., Querol, X., Alastuey, A., Cusack, M., and Reche, C.: Intense winter atmospheric pollution episodes affecting the Western Mediterranean., Sci. Total Environ., 408, 1951–1959, doi:10.1016/j.scitotenv.2010.01.052, 2010a.

Pey, J., Querol, X., and Alastuey, A.: Discriminating the regional and urban contributions in the North-Western Mediterranean: PM levels and composition, Atmos. Environ., 44, 1587–1596, doi:10.1016/j.atmosenv.2010.02.005, 2010b.

Pey, J., Querol, X., Alastuey, A., Forastiere, F., and Stafoggia, M.: African dust outbreaks over the Mediterranean Basin during 2001–2011: $PM_{10}$ concentrations, phenomenology and trends, and its relation with synoptic and mesoscale meteorology, Atmos. Chem. Phys., 13, 1395–1410, doi:10.5194/acp-13-1395-2013, 2013.

Pope III, C. A. and Dockery, D. W.: Health effects of fine particulate air pollution: Lines that connect, J. Air Waste Manage., 56, 709–742, 2006.

Putaud, J. P., Van Dingenen, R., Alastuey, A., Bauer, H., Birmili, W., Cyrys, J., Flentje, H., Fuzzi, S., Gehrig, R., Hansson, H. C., Harrison, R. M., Herrmann, H., Hitzenberger, R.,





ACPD
13, 27201–27241, 2013



Hüglin, C., Jones, A. M., Kasper-Giebl, A., Kiss, G., Kousa, A., Kuhlbusch, T. A. J., Löschau, G., Maenhaut, W., Molnar, A., Moreno, T., Pekkanen, J., Perrino, C., Pitz, M., Puxbaum, H., Querol, X., Rodriguez, S., Salma, I., Schwarz, J., Smolik, J., Schneider, J., Spindler, G., Ten Brink, H., Tursic, J., Viana, M., Wiedensohler, A., and Raes, F.: A European aerosol phenomenology – 3: Physical and chemical characteristics of particulate matter from 60 rural, urban, and kerbside sites across Europe, Atmos. Environ., 44, 1308–1320, 2010.

Querol, X., Alastuey, A., Lopez-Soler, A., Plana, F., and Puicercus, J. A.: Daily evolution of sulphate aerosols in a rural area, northeastern Spain – elucidation of an atmospheric reservoir effect, Environ. Pollut., 105, 397–407, doi:10.1016/S0269-7491(99)00037-8, 1999.

Querol, X., Alastuey, A., Pey, J., Cusack, M., Pérez, N., Mihalopoulos, N., Theodosi, C., Gerasopoulos, E., Kubilay, N., and Koçak, M.: Variability in regional background aerosols within the Mediterranean, Atmos. Chem. Phys., 9, 4575–4591, doi:10.5194/acp-9-4575-2009, 2009.

Reche, C., Viana, M., Moreno, T., Querol, X., Alastuey, A., Pey, J., Pandolfi, M., Prévôt, A., Mohr, C., Richard, A., Artiñano, B., Gomez-Moreno, F. J., and Cots, N.: Peculiarities in atmospheric particle number and size-resolved speciation in an urban area in the western Mediterranean: Results from the DAURE campaign, Atmos. Environ., 45, 5282–5293, doi:10.1016/j.atmosenv.2011.06.059, 2011.

Rodríguez, S., Querol, X., Alastuey, A., Viana, M.-M., and Mantilla, E.: Events affecting levels and seasonal evolution of airborne particulate matter concentrations in the Western Mediterranean., Environ. Sci. Technol., 37, 216–22, 2003.

Rodríguez, S., Alastuey, A., Alonso-Pérez, S., Querol, X., Cuevas, E., Abreu-Afonso, J., Viana, M., Pérez, N., Pandolfi, M., and de la Rosa, J.: Transport of desert dust mixed with North African industrial pollutants in the subtropical Saharan Air Layer, Atmos. Chem. Phys., 11, 6663–6685, doi:10.5194/acp-11-6663-2011, 2011.

Seco, R., Peñuelas, J., Filella, I., Llusià, J., Molowny-Horas, R., Schallhart, S., Metzger, A., Müller, M., and Hansel, A.: Contrasting winter and summer VOC mixing ratios at a forest site in the Western Mediterranean Basin: the effect of local biogenic emissions, Atmos. Chem. Phys., 11, 13161–13179, doi:10.5194/acp-11-13161-2011, 2011.

Tositti, L., Riccio, A., Sandrini, S., Brattich, E., Baldacci, D., Parmeggiani, S., Cristofanelli, P., and Bonasoni, P.: Short-term climatology of $PM_{10}$ at a high altitude background station in southern Europe, Atmos. Environ., 65, 142–152, doi:10.1016/j.atmosenv.2012.10.051, 2013.





ACPD
13, 27201–27241, 2013



Venzac, H., Sellegri, K., Villani, P., Picard, D., and Laj, P.: Seasonal variation of aerosol size distributions in the free troposphere and residual layer at the puy de Dôme station, France, Atmos. Chem. Phys., 9, 1465–1478, doi:10.5194/acp-9-1465-2009, 2009.

Vrekoussis, M., Liakakou, E., Koçak, M., Kubilay, N., Oikonomou, K., Sciare, J., and Mihalopoulos, N.: Seasonal variability of optical properties of aerosols in the Eastern Mediterranean, Atmos. Environ., 39, 7083–7094, doi:10.1016/j.atmosenv.2005.08.011, 2005.

WHO, World Health Organisation, Regional Office for Europe: Review of evidence on health aspects of air pollution – REVIHAAP – first results, WHO Regional Office for Europe, Scherfigsvej 8, 2100 Copenhagen Ø, Denmark, 2013.

Zieger, P., Kienast-Sjögren, E., Starace, M., von Bismarck, J., Bukowiecki, N., Baltensperger, U., Wienhold, F. G., Peter, T., Ruhtz, T., Collaud Coen, M., Vuilleumier, L., Maier, O., Emili, E., Popp, C., and Weingartner, E.: Spatial variation of aerosol optical properties around the high-alpine site Jungfraujoch (3580 m a.s.l.), Atmos. Chem. Phys., 12, 7231–7249, doi:10.5194/acp-12-7231-2012, 2012.





ACPD
13, 27201–27241, 2013



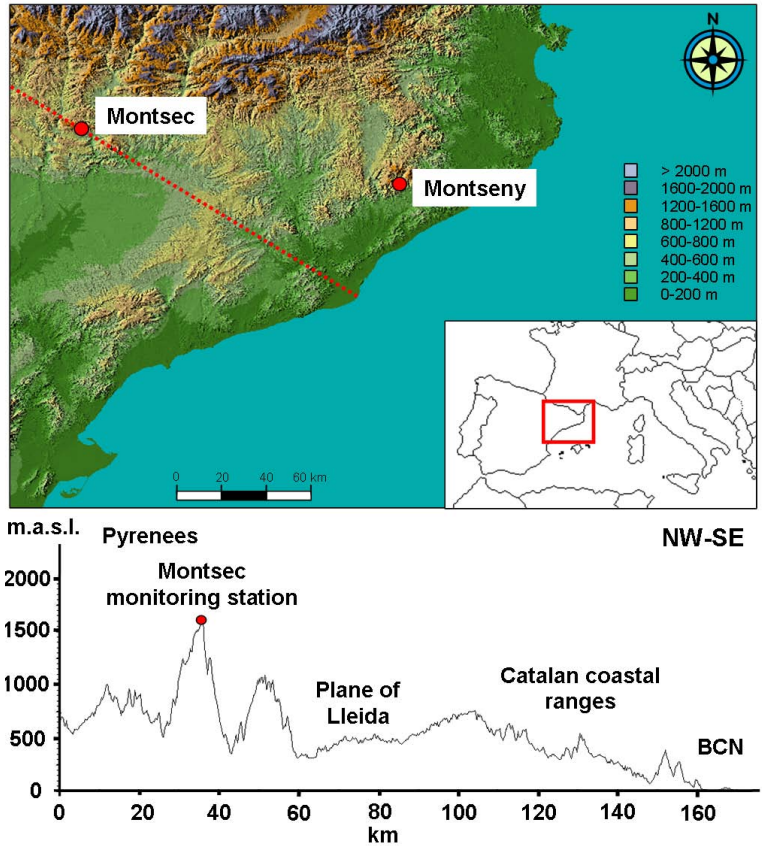


**Fig. 1.** Top: location of the two monitoring stations (Montsec and Montseny). Bottom: topography of the Montsec area.





ACPD
13, 27201–27241, 2013



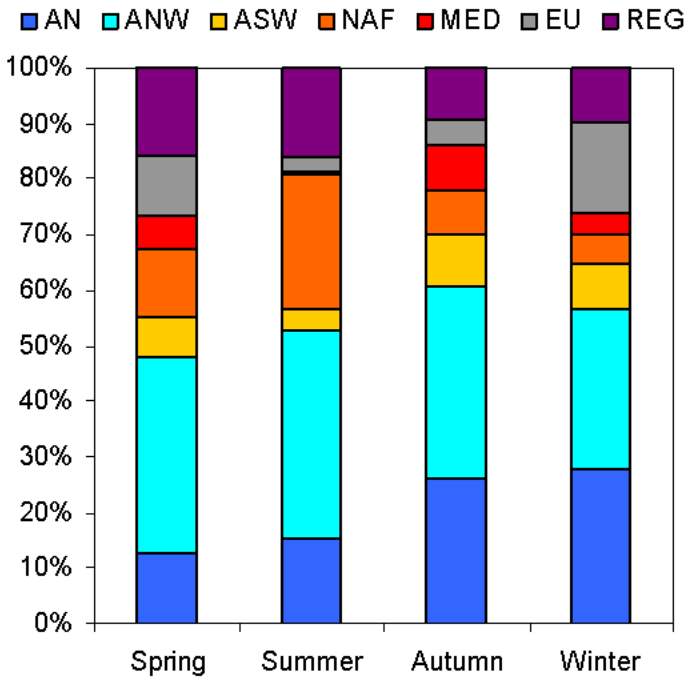


**Fig. 2.** Frequency of air mass origin as a function of season at Montsec.





ACPD
13, 27201–27241, 2013



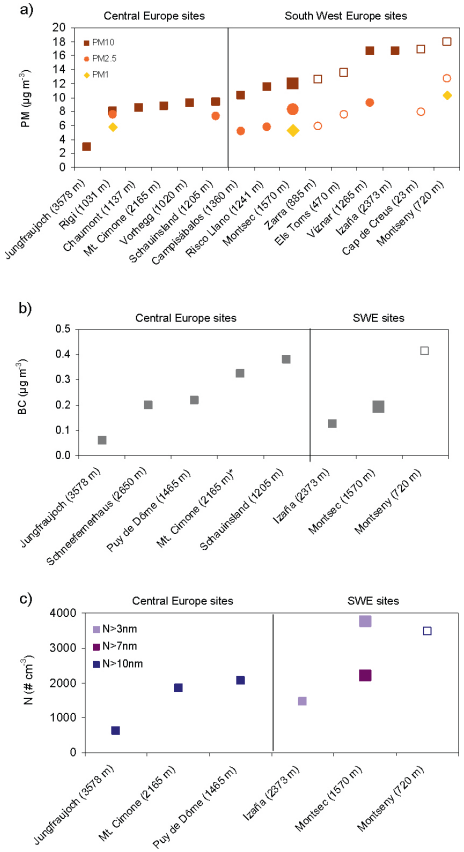


**Fig. 3.** Mean concentrations of **(a)** PM, **(b)** BC and **(c)** *N* during the study period compared with the data available in the ACTRIS Data Center web site. * Mt.Cimone BC concentrations averaged from 2007 to 2009. Non solid markers correspond to non high altitude sites.





ACPD
13, 27201–27241, 2013



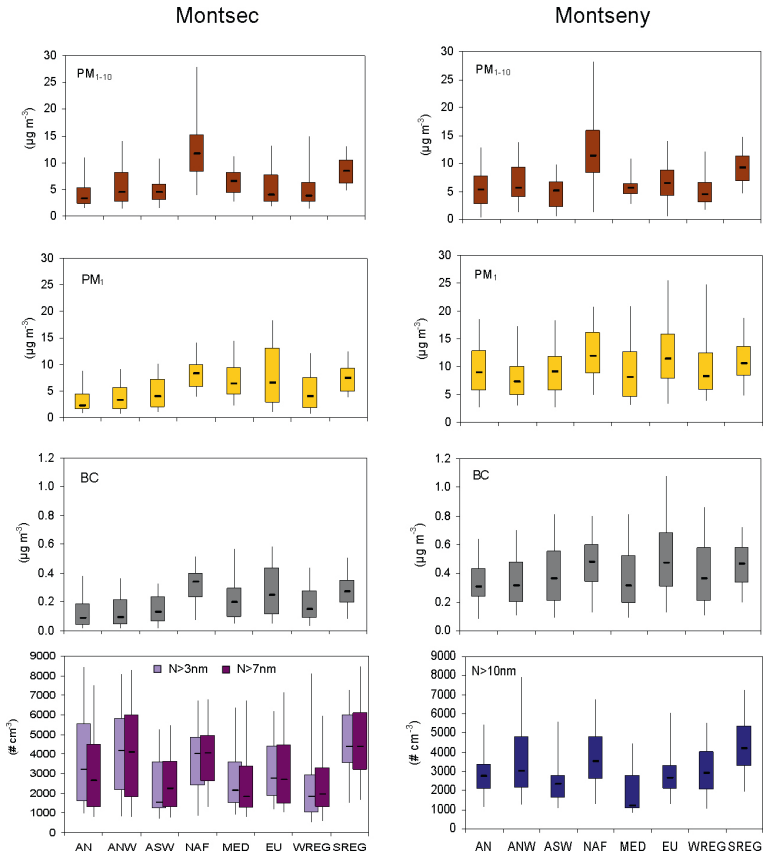


**Fig. 4.** Median (black line within the boxes) and percentiles (5–25–75–95, boxes and whiskers) of daily $PM_{1-10}$, $PM_1$, BC and *N* concentrations during the study period as a function of the air mass origin at Montsec and Montseny.





ACPD
13, 27201–27241, 2013



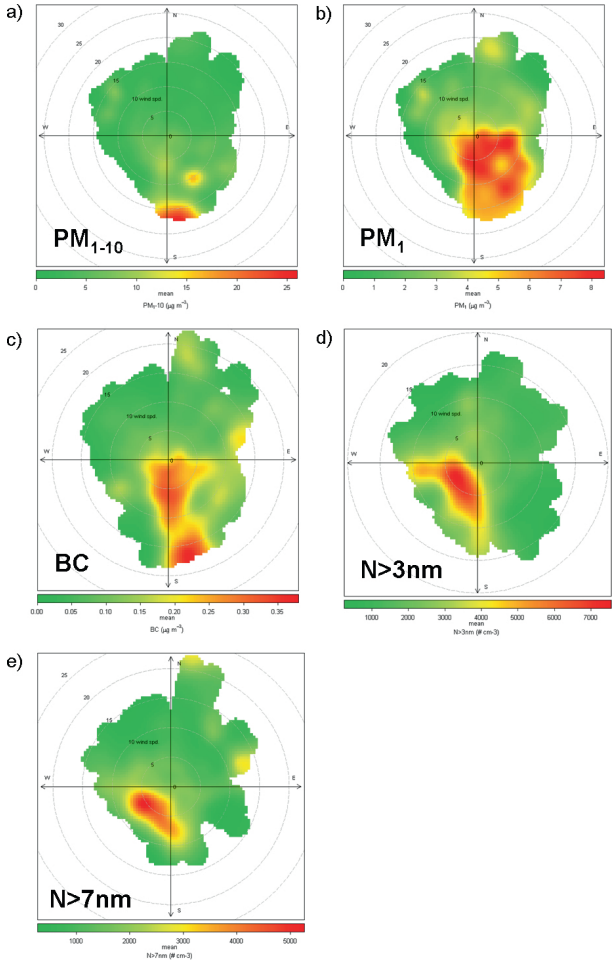


**Fig. 5.** Hourly concentrations of **(a)** $PM_{1-10}$, **(b)** $PM_1$, **(c)** BC, **(d)** $N > 3$ nm and **(e)** $N > 7$ nm during the study period as a function of the wind speed and direction at Montsec.





ACPD
13, 27201–27241, 2013

Aerosol mass, black carbon and particle number concentrations

A. Ripoll et al.



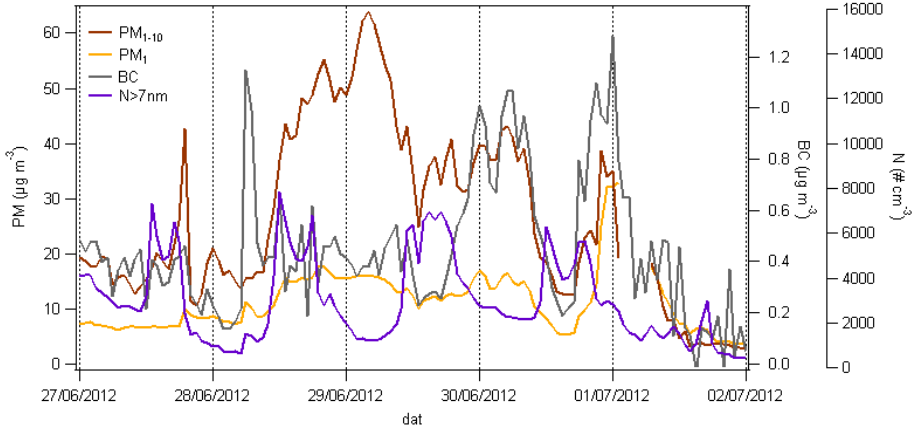


**Fig. 6.** Time series of $PM_{1-10}$, $PM_1$, BC and *N* concentrations under Saharan dust intrusion and wildfire episode affecting Montsec area.





ACPD
13, 27201–27241, 2013



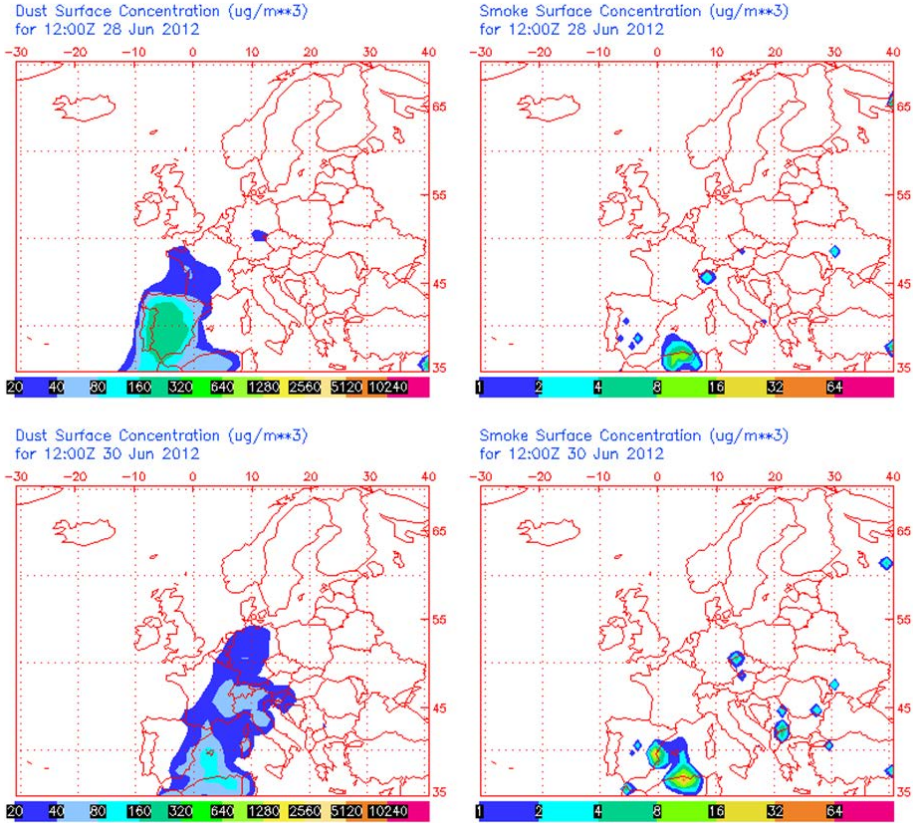


**Fig. 7.** Dust and smoke surface concentration from the NAAPS model under Saharan dust intrusion and wildfire episode affecting Montsec area.





ACPD
13, 27201–27241, 2013



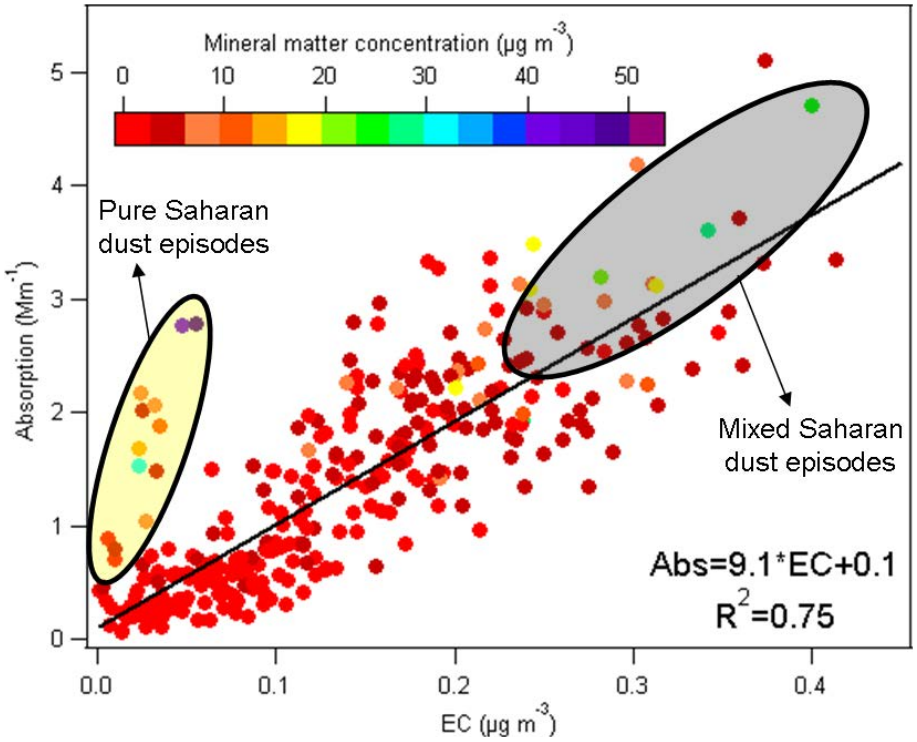


**Fig. 8.** Measured absorption versus $PM_{10}$ elemental carbon (EC) concentration as a function of $PM_{10}$ mineral matter concentration during the study period at Montsec.





ACPD
13, 27201–27241, 2013



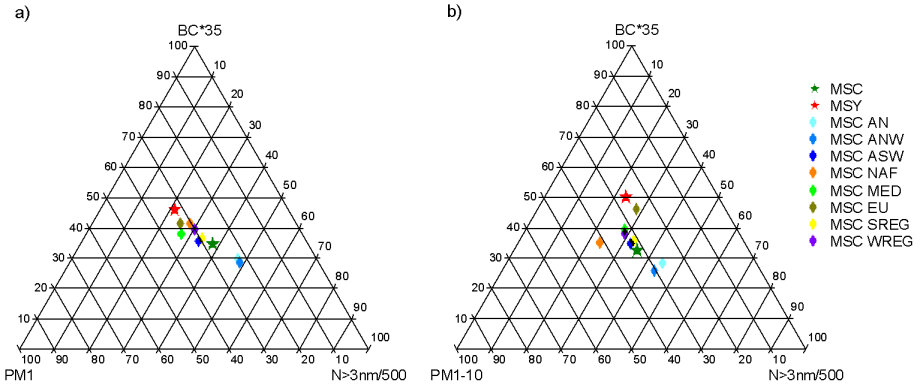


**Fig. 9.** Ternary Plot of **(a)** $PM_1$, $BC * 35$ and $N > 3\,nm/500$, and **(b)** $PM_{1-10}$, $BC * 35$ and $N/500$ mean concentrations at Montsec and Montseny, and mean concentrations as a function of air mass origin at Montsec during the study period.





ACPD
13, 27201–27241, 2013



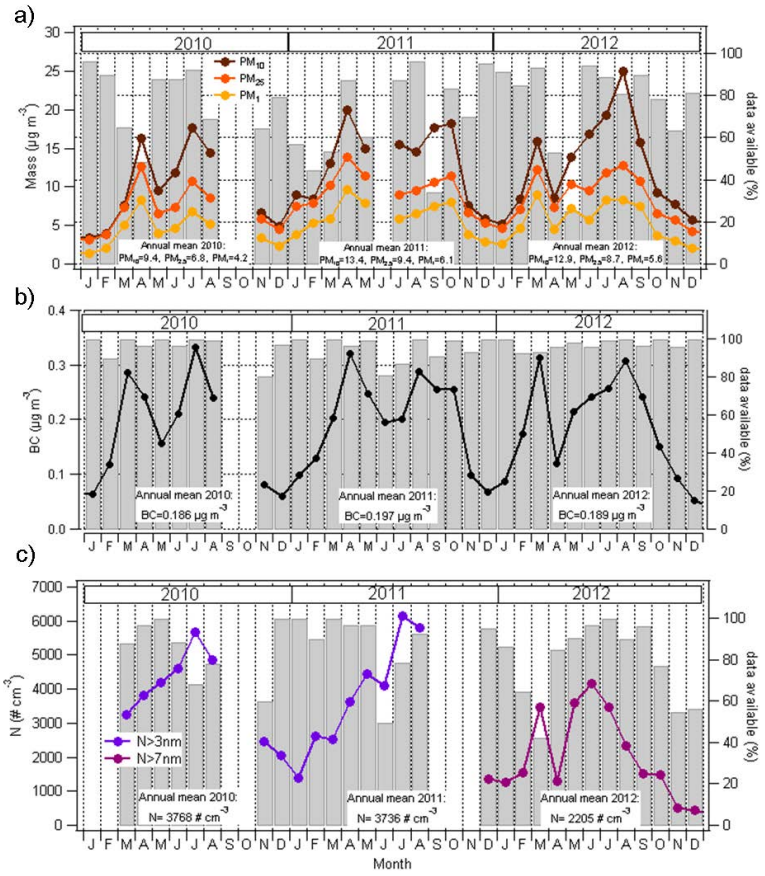


**Fig. 10.** Time series of monthly averaged **(a)** PM, **(b)** BC, and **(c)** *N* measured at Montsec.





ACPD
13, 27201–27241, 2013



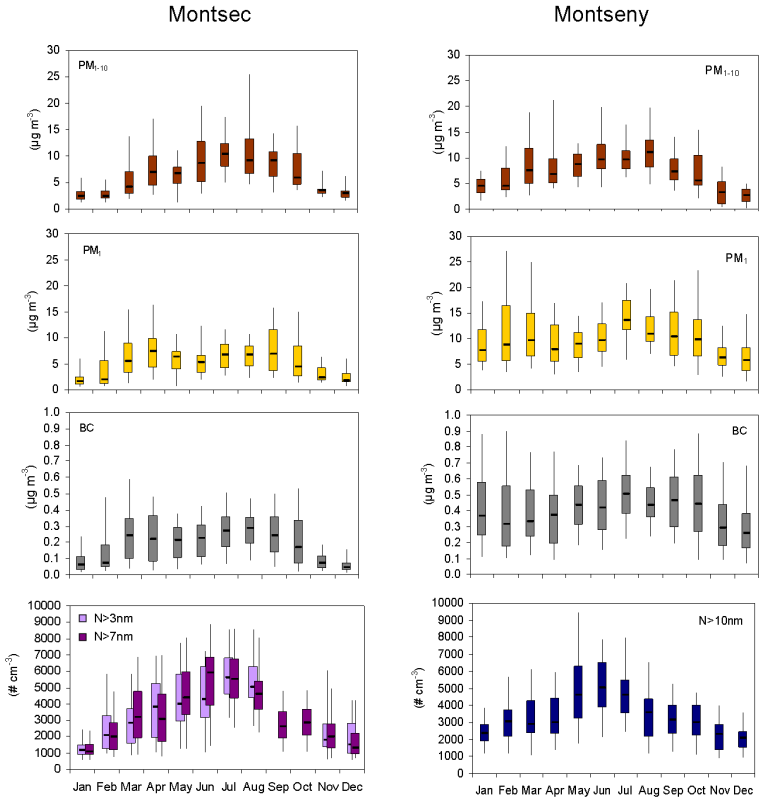


**Fig. 11.** Monthly median (black line within the boxes) and percentiles (5–25–75–95, boxes and whiskers) of daily $PM_{1-10}$, $PM_1$, BC and *N* concentrations during the study period at Montsec and Montseny sites.





ACPD
13, 27201–27241, 2013



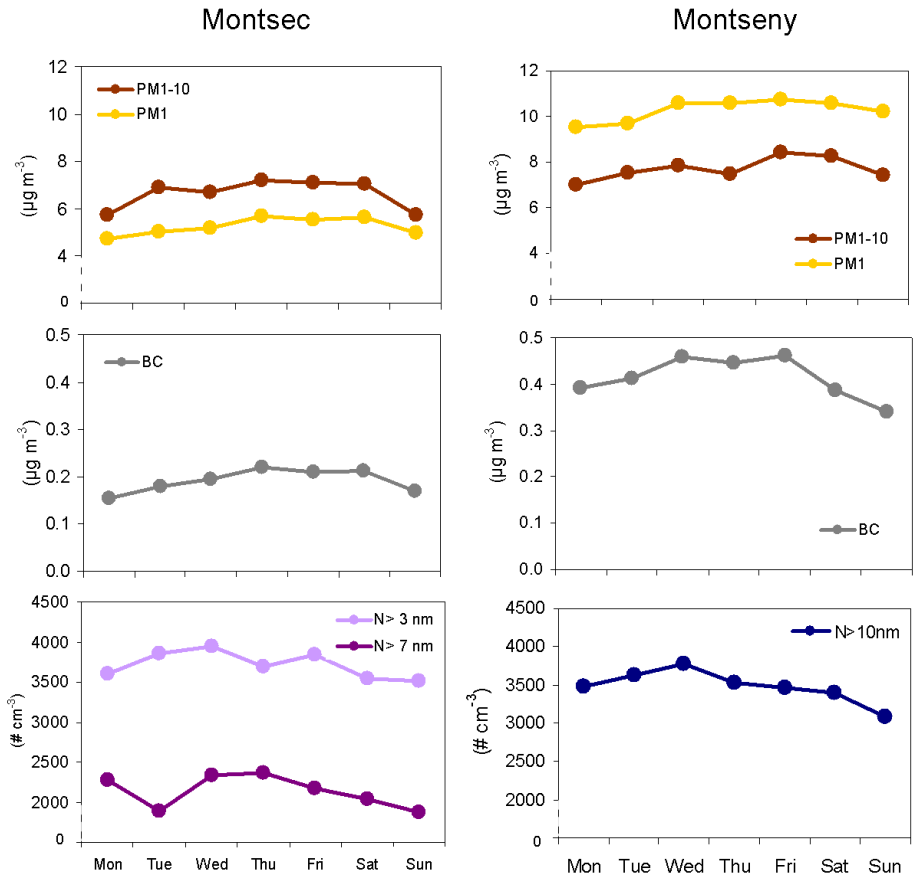


**Fig. 12.** Weekly cycles of daily PM, BC and *N* concentration during the study period at Montsec and Montseny.





ACPD
13, 27201–27241, 2013



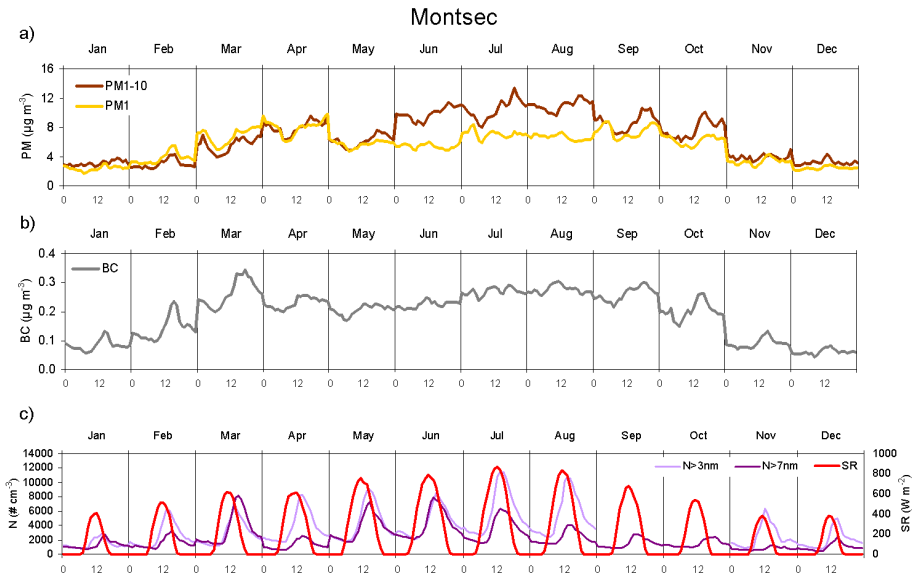


**Fig. 13.** Daily patterns of hourly **(a)** $PM_1$, $PM_{1-10}$, **(b)** BC, **(c)** $N > 3$ nm, $N > 7$ nm and solar radiation measurements averaged for each month during the study period at Montsec.





ACPD
13, 27201–27241, 2013